

## Guest Inclusion Properties of Calix[6]arene-based Unimolecular Cage Compounds. On Their High Cs<sup>+</sup> and Ag<sup>+</sup> Selectivity and Very Slow Metal Exchange Rates

Hideyuki Otsuka,<sup>†</sup> Yoshio Suzuki,<sup>†</sup> Atsushi Ikeda,<sup>†</sup> Koji Araki,<sup>‡</sup> and Seiji Shinkai<sup>\*†</sup>

Department of Chemical Science & Technology, Faculty of Engineering, Kyushu University, Higashi-ku, Fukuoka 812, Japan

Department of Chemistry, Kyushu Institute of Technology, Tobata-ku, Kitakyushu 804, Japan

Received 29 September 1997; accepted 22 October 1997

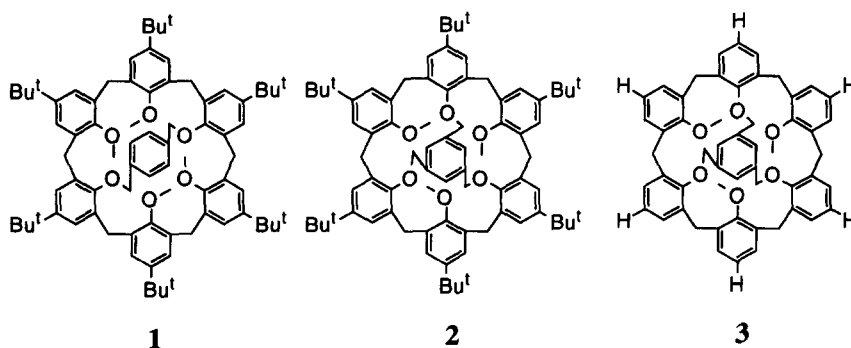
**Abstract:** The reaction of 1,3,5-tri-*O*-alkylated calix[6]arenes with 1,3,5-tris(bromomethyl)benzene yielded capped calix[6]arenes (**2** with *tert*-butyl groups on the upper rim and **3** without *tert*-butyl groups) in unexpectedly high yields (80 - 91%). Combined studies of **2** and **3** by MM3 computation, X-ray analysis, and <sup>1</sup>H NMR spectroscopy established that these calix[6]arenes feature a unique structure consisting of alternately-arranged three flattened mesitylene-linked phenyl units and three stand-up anisole units. Particularly, compound **2** possesses a closed ionophoric cavity: the upper hemisphere is closed by three *tert*-butyl groups of anisole units and the lower hemisphere is closed by a mesitylene cap and three anisole methoxy groups. The <sup>1</sup>H NMR spectrum was scarcely changed at wide temperature range (30 ~ 130 °C), indicating that the structure is extremely rigidified. Both solvent extraction and spectroscopic studies established that this cavity shows the high selectivity toward Cs<sup>+</sup> among alkali metal cations, the high affinity with Ag<sup>+</sup>, and the moderate affinity with RNH<sub>3</sub><sup>+</sup>. *Very surprisingly, the association-dissociation processes for 2 and cesium picrate was so slow that the rate could be followed by a conventional spectroscopic method.* The thermodynamic parameters determined by kinetic studies disclosed that the major driving-force for Cs<sup>+</sup> inclusion is the entropy term based on the desolvation.  
© 1997 Elsevier Science Ltd. All rights reserved.

### INTRODUCTION

Calix[*n*]arenes are cyclic oligomers that belong to the class of [1<sub>*n*</sub>]-metacyclophanes. As calix[*n*]arenes have a cavity-shaped architecture, they are useful as building blocks for host-guest-type receptors and catalysts through appropriate modification.<sup>1</sup> Functional groups can be introduced either to the upper rim by means of electrophilic substitution reactions<sup>1-5</sup> or to the lower rim by means of Williamson-type OH-modifications.<sup>1,6-12</sup> Among them the π-basic cavity of calix[4]arenes seems to be too small to accept organic host molecules whereas those of calix[6]arenes and calix[8]arenes seem to be large enough to include them but are too flexible to show guest selectivity. To precisely recognize organic guest molecules, it is no doubt that the receptor cavity should be "moderately" rigid and well delineated by functional groups. Since calix[*n*]arenes have the rotational freedom about their phenyl units,<sup>1</sup> it seems indispensable to suppress this rotational freedom in order to enjoy molecular design in calix[*n*]arene-based host-guest chemistry. It is now possible to suppress the rotation of phenyl units in calix[4]arenes by introduction of bulky *O*-substituents,<sup>1,9,13</sup> but in larger calix[6]arenes and calix[8]arenes it is

still a difficult job. Gutsche et al.<sup>2c</sup> previously described that "even the calix[6]arenes are rather flexible and further insight into their mode of action must await the construction of more rigid and conformationally-defined analogs".

More recently, it was shown that the phenyl unit rotation in calix[6]arenes can be suppressed by the multi-point bridging of the lower rim. In 1993, Biali et al.<sup>14</sup> succeeded in the immobilization using two dialkylphosphates which can react with six phenol groups. Gutsche et al.<sup>15</sup> synthesized compound **1** in which the 1,4-phenyl units are bridged by a xylenyl unit; **1** is capable of undergoing a conformational transformation in which the bridging moiety becomes threaded through the annulus to produce a "self-anchored rotaxane". We synthesized triply-bridged calix[6]arenes at the upper-rim side or at the lower-rim side via complicated synthetic routes.<sup>16</sup> Although ring inversion is permanently suppressed in these calix[6]arenes, the influence of the conformation immobilization on the inclusion properties is little understood so far. To obtain further insights into the relation between the ring inversion and the bridging effect, we synthesized triply-bridged (i.e., "capped") **2**<sup>17</sup> and **3**. The capping of 1,3,5-tri-*O*-alkylated calix[6]arenes with 1,3,5-tris(bromomethyl)benzene gave the products in unexpectedly high yields (80-91%).<sup>17</sup> The high yields were accounted for by the advantage in C<sub>3</sub>-symmetrical complementarity between these two reactants.<sup>17</sup> In these capped products, ring inversion was inhibited under the present measurement conditions,<sup>18</sup> and the presence of a closed inner cavity was suggested on the basis of <sup>1</sup>H NMR spectroscopy and MM3 calculations.<sup>17b</sup> The purpose of the present study is to thoroughly characterize the inclusion properties of this unique cavity composed of seven benzene rings and six ethereal oxygens.<sup>19</sup> We have found that the cavity shows very high Cs<sup>+</sup> and Ag<sup>+</sup> affinity and the association-dissociation rates are so slow as to be measurable by a conventional spectroscopic method.



## RESULTS AND DISCUSSION

**Combined Studies on the Structure of 2 and 3 by MM3(92) Computation, X-ray Crystallographic Analysis, and  $^1\text{H}$  NMR Spectroscopy.**

It has been shown that the structural characteristics of calix[n]arene derivatives are satisfactorily reproduced using MM3(92).<sup>20</sup> Judging from the CPK model building, the basic skeletons of **2** and **3** are very rigid and can adopt only a few limited conformations. This situation is very suitable to the theoretical prediction of the energy-minimized structures. They are shown in Figs. 1 and 2. It is clearly seen from Fig. 1 that in **2** the lower rim is covered by a mesitylene cap and three methoxy groups whereas the upper rim is covered by three alternate *tert*-butyl groups. Three phenyl units linked to the mesitylene cap are considerably flattened ( $50.9^\circ$  to the least-squares plane of six  $\text{ArCH}_2\text{Ar}$  methylene carbons). In contrast, residual three anisole units stand up ( $105.4^\circ$ ). These angles can assemble six *tert*-butyl groups on the upper rim and three of them in the linked phenyl units occupy an exterior space and three of them in the anisole units occupy an interior space. The latter three *tert*-butyl groups apparently act as a lid of the upper rim edge. The cross-section of the inner cavity thus constructed is shown in Fig. 3. It is seen from Figs. 1 and 3 that three benzene rings in the anisole units and one benzene ring in the mesitylene cap are arranged in a nearly tetrahedral architecture and lone-pair electrons in three oxygen atoms connected to the mesitylene cap are directed toward the inside of the cavity. The results suggest that this cavity should be highly electron-rich. In contrast, the upper rim edge of compound **3** which does not have *tert*-butyl groups on the upper rim is not closed (see the right picture in Fig. 2). Careful comparison of Fig. 2 with Fig. 1 reveals that three alternate phenyl

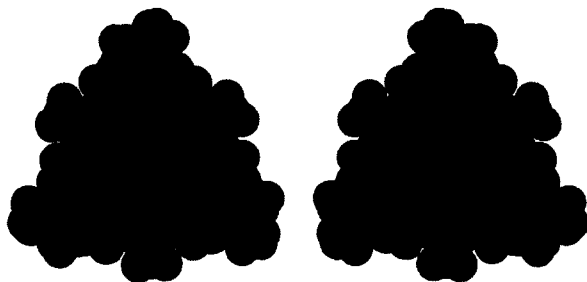


**Fig. 1.** Energy-minimized structure of **2**: bottom view from the mesitylene-capped lower rim (left) and top view from the upper rim covered by three alternate *tert*-butyl groups (right).

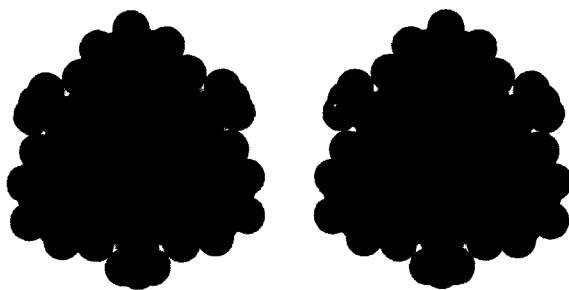


**Fig. 2.** Energy-minimized structure of **3**: bottom view (left) and top view (right).

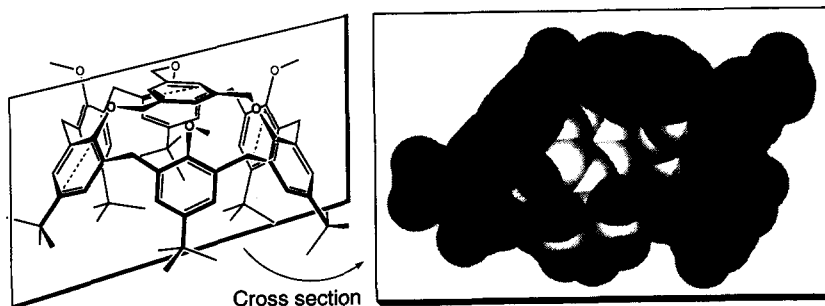


**Fig. 3.** An electron-rich inner cavity of **2** visualized by the cross-section.

units linked to the mesitylene cap in **3** are more flattened ( $26.1^\circ$ ) than those in **2**. Furthermore, examination of Fig. 2 reveals that the crank-shaft-like structure of three Ar(cap)-CH<sub>2</sub>-O-Ar(calix) linkages in **2** exists nearly in the same plane as the mesitylene cap whereas that in **3** is rather perpendicular to the mesitylene cap. Presumably, the mesitylene cap in **2** is twisted to reduce the steric crowding among six *tert*-butyl groups on the upper rim.

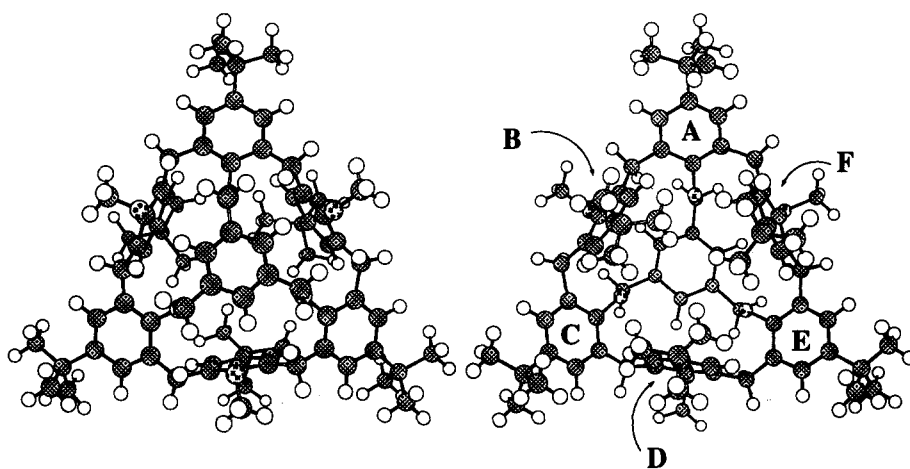


**Fig. 4.** X-ray structure of **2**: bottom view from the mesitylene-capped lower rim (left) and top view from the upper rim covered by three alternate *tert*-butyl groups (right).

The X-ray structure of **2** is shown in Fig. 4. The X-ray structures of *O*-alkylated calix[6]arene derivatives reported so far are those of 1,2,3-alternate (i.e., **uuuddd**) isomers.<sup>21</sup> In this context this is a rare example for the X-ray structure of an *O*-alkylated calix[6]arene with a cone-like conformation. It is clearly seen from Fig. 4 that the angles for six benzene rings change alternately. Flattened A, C, and E phenyl units have the angles of 20.04°, 22.59°, and 21.93°, respectively whereas stand-up B, D, and F anisole units have the angles of 100.96°, 102.62°, and 103.47°, respectively, with respect to the least-squares plane of six ArCH<sub>2</sub>Ar methylene carbons. The angles predicted from the MM3 calculation are 50.9° for the flattened phenyl units and 105.4° for the stand-up anisole units. The angle for the stand-up anisole units well coincides with that predicted from the MM3 calculation, but that for the flattened phenyl units is smaller by ca. 30°. This discordance is related to the difference in the structure of the crank-shaft-like linkage in the Ar(cap)-CH<sub>2</sub>-O-Ar(calix) moieties: in the energy-minimized structure these linkages exist nearly in the same plane as the mesitylene cap whereas in the X-ray structure they are nearly perpendicular to the mesitylene cap. Presumably, **2** in the single crystal is enforced to adopt a more flattened conformation in order to be packed in the crystal lattice. Comparison of these two structures reveals that the more flattened the phenyl units are, the more perpendicular the Ar(cap)-CH<sub>2</sub>-O-Ar(calix) linkages become and the lone-pair electrons of three oxygens are more directed toward the inside of the cavity. The inner cavity size (3.2 - 4.0 Å between the upper rim and the lower rim<sup>22</sup>; 5.0 Å between the distal benzene rings) is nearly the same between these two structures. Since this size is slightly larger than the diameter of Cs<sup>+</sup> (3.62 Å), it is predictable that this cavity would show high Cs<sup>+</sup> selectivity among alkali metal cations. The open space at the upper rim, through which metal cations are associated or dissociated, is very narrow. A triangle formed from three *tert*-carbons in the *tert*-butyl groups of anisole units consists of three sides with 5.89, 5.99, and 6.23 Å and the diameter of an inscribed circle is 3.48 Å. Since this diameter is slightly smaller than that of Cs<sup>+</sup>, one may expect some interference with the association and dissociation of Cs<sup>+</sup>.

The temperature-dependent <sup>1</sup>H NMR spectra of **2** showed that a pair of doublets for the ArCH<sub>2</sub>Ar protons consistently appears from -85 °C to 130 °C (Fig. 5). The result indicates that **2** firmly maintains a cone conformation. However, this fact is not sufficient to propose the permanent freezing of this conformation, because the rate of cone-cone ring inversion may be only slower than the NMR time-scale.<sup>17,18,21,23</sup> The direct evidence for immobilization was obtained from 2D EXSY (Bruker ARX-300 instrument, NOESYTP with time proportional phase increment; [2] = 10 mmol dm<sup>-3</sup>, Cl<sub>2</sub>CDCDCl<sub>2</sub>, τ<sub>m</sub> 800 ms) in <sup>1</sup>H NMR spectroscopy<sup>16,23</sup>; at 30 - 130 °C the correlation arising from the exchange between H<sub>ax</sub> and H<sub>eq</sub> in the ArCH<sub>2</sub>Ar methylene protons was not observed. The result reveals that **2** is immobilized in a cone conformation and flip-flop-type ring inversion does not take place under the present measurement conditions.

Previously, Casnati et al.<sup>7c</sup> and Duynhoven et al.<sup>24</sup> synthesized a number of 1,3,5-tri-*O*-substituted calix[6]arene derivatives (**4**). In these molecules the δ<sub>H</sub> values for the methoxy protons appear at higher magnetic field (2.15-2.31 ppm), indicating that these methoxy groups are flattened into the cavity. We synthesized a

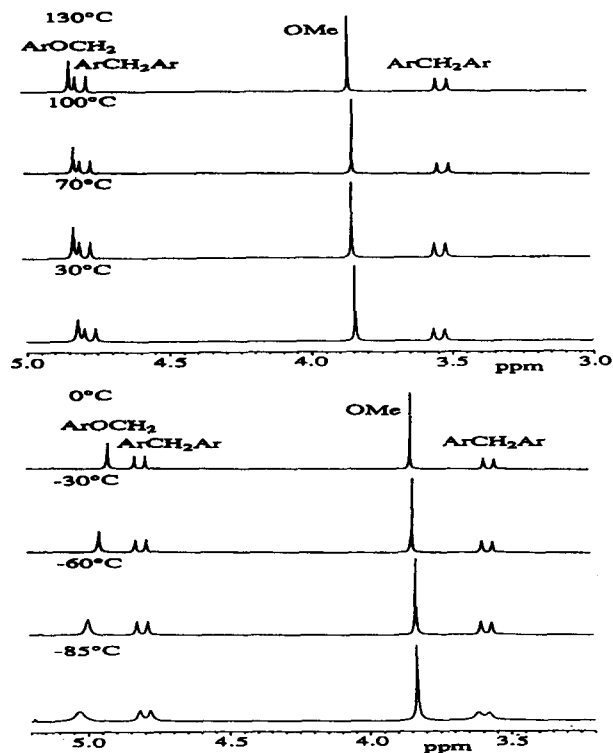
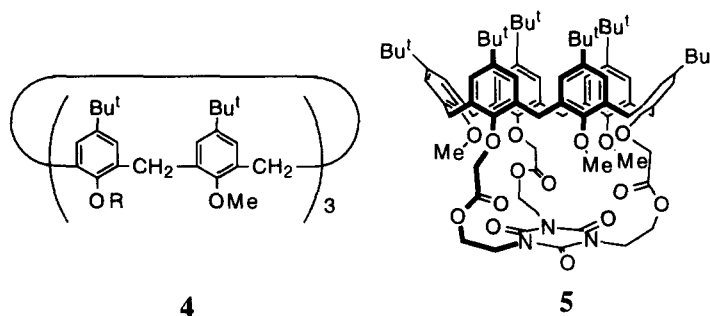


**Fig. 5.** Temperature dependence of  $^1\text{H}$  NMR spectra for **2** (400 MHz,  $\text{CD}_2\text{Cl}_2$  below  $0^\circ\text{C}$  and  $\text{Cl}_2\text{CDCDCl}_2$  above  $30^\circ\text{C}$ ).

triply-capped calix[6]arene (**5**).<sup>16a,25</sup> The  $\delta_{\text{H}}$  value for the methoxy protons appears at higher magnetic field (2.69 ppm) again, indicating that **5** adopts a conformation similar to **4** including flattened anisole units. In contrast, the  $\delta_{\text{H}}$  for the methoxy protons in **2** appears at relatively lower magnetic field (3.85 ppm). The  $\delta_{\text{H}}$  values for the *tert*-butyl protons in anisole units and linked phenyl units appear at 0.72 and 1.41 ppm, respectively; the shifts of these protons are opposite to those in **4** and **5** (1.24–1.47 ppm for the *tert*-butyl protons in anisole units and 0.71–0.94 ppm for those in linked phenyl units). The results indicate that in **2** linked phenyl units are flattened and anisole units rather stand up. The alternately flattened and stand-up structure substantiated by  $^1\text{H}$  NMR spectroscopy is in good agreement with those shown by theoretical calculations (Fig. 1) and X-ray analysis (Fig. 4). On the other hand, the energy-minimized structure in Fig. 1 clearly indicates that two  $\text{OCH}_2$  methylene protons are inequivalent to each other. Although the inequivalency in the X-ray structure is not so clear as that in the energy-minimized structure, the unsymmetrically-bent  $\text{Ar}(\text{cap})\text{-CH}_2\text{-O-Ar}(\text{calix})$  linkages suggest that the two  $\text{OCH}_2$  methylene protons can be basically inequivalent. These structural characteristics

imply that they may appear as a pair of doublets in  $^1\text{H}$  NMR spectroscopy. As seen from Fig. 5, however, they appear as a singlet resonance even at  $-85\text{ }^\circ\text{C}$ . The result implies that even though the mesitylene cap occupies an unsymmetrical position, the right turn-left turn twisting motion occurs faster than the NMR time-scale. The  $\text{OCH}_2$  methylene protons in **3** also appeared as a singlet resonance.

The foregoing results indicate that MM3-based theoretical calculations, X-ray analysis, and  $^1\text{H}$  NMR spectroscopy all support the structural characteristics of **2** with a unique unimolecularly-closed inner cavity. Next, we estimated the guest-binding properties of this ionophoric cavity.



**Two-phase Solvent Extraction and Determination of Association Constants by Spectroscopic Methods.** It has been shown by Ungaro et al.,<sup>7b,26</sup> McKervey et al.,<sup>10,11</sup> Chang et al.,<sup>27</sup> and others<sup>12,28</sup> that calix[n]arenes can be derived to neutral ligands by introduction of ester or amide groups into OH groups. They demonstrated that the metal selectivity is dependent on the calix[n]arene ring size: that is, calix[4]aryl derivatives show very high  $\text{Na}^+$  selectivity whereas calix[6]aryl and calix[8]aryl derivatives rather show broad alkali metal affinity with  $\text{K}^+$ ,  $\text{Rb}^+$ , and  $\text{Cs}^+$ .<sup>1,7,10,11,26-28</sup> This is related to the ring flexibility inherent to calix[6]arene and calix[8]arene, which inevitably features the induced-fit-type metal complexation. In contrast, the NMR spectral data for **2** indicate that the framework is considerably rigidified and possibly shows high metal selectivity. Judging from the theoretical calculations that the size of the inner cavity ( $3.2 \sim 4.0 \times 5.0 \text{ \AA}$ )<sup>22</sup> is comparable with the diameter of  $\text{Cs}^+$  ( $3.62 \text{ \AA}$ ), one can expect that this cavity shows high selectivity toward  $\text{Cs}^+$  over other alkali metal cations.

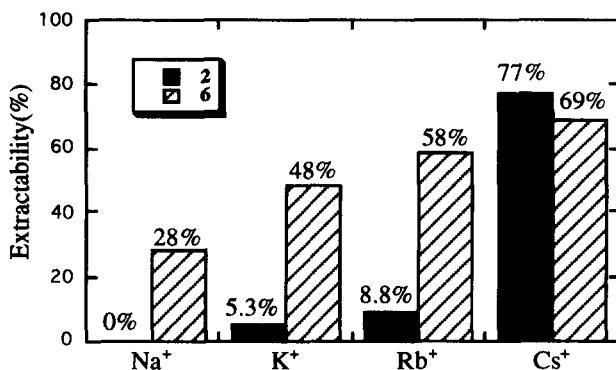
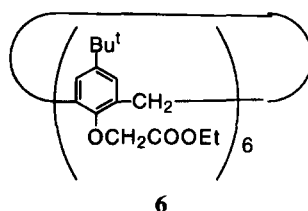


**Fig. 6.** Percent extraction of alkali picrates in dichloromethane at 25 °C (for the details of the extraction conditions see Experimental Section).

Solvent extraction of alkali metal cations with picrate ion into dichloromethane was performed at 25 °C (for the details of the extraction conditions see Experimental Section). The extractability values (Ex%) are compared with those of conformationally-mobile calix[6]arylester **6** (Fig. 6). It is clearly seen from Fig. 6 that **6** shows the broad affinity with alkali metal cations whereas **2** shows high selectivity toward Cs<sup>+</sup> over other alkali metal cations: it extracts Rb<sup>+</sup> and K<sup>+</sup> only to a smaller extent and shows no affinity with Na<sup>+</sup>.

**Table 1.** Bathochromic Shifts ( $\lambda_{\max}$ ) of Alkali Picrates Extracted into the Dichloromethane Phase<sup>a</sup>

ionophore	$\lambda$ (nm)			
	M <sup>+</sup> = Na <sup>+</sup>	K <sup>+</sup>	Rb <sup>+</sup>	Cs <sup>+</sup>
18-crown-6 <sup>b</sup>	367	369	368	369
[2,2,1]cryptand <sup>b</sup>	375	375	375	375
[2,2,2]cryptand <sup>b</sup>	375	375	375	376
<b>2</b>	377	378	378	378

<sup>a</sup> 25 °C

<sup>b</sup> Cited from Ref. 29.

**Table 2.** Association Constants of **2** with Alkali Metal Cations and RNH<sub>3</sub><sup>+</sup>Pic<sup>-a</sup>

guest	$K_{\text{ass}} / \text{M}^{-1}$
<b>M<sup>+</sup>Pic<sup>-</sup></b>	
M <sup>+</sup> = Na <sup>+</sup>	< 20
K <sup>+</sup>	< 20
Rb <sup>+</sup>	ca. 20
Cs <sup>+</sup>	21000
<b>RNH<sub>3</sub><sup>+</sup>Pic<sup>-</sup></b>	
R = Me	14400
Et	11400
<i>n</i> -Pr	8000
<i>n</i> -Bu	1500
<i>iso</i> -Bu	3300
<i>sec</i> -Bu	500
<i>tert</i> -Bu	500

<sup>a</sup> THF for M<sup>+</sup>Pic<sup>-</sup> and CHCl<sub>3</sub> : THF = 99 : 1 v/v for RNH<sub>3</sub><sup>+</sup>Pic<sup>-</sup>

Inoue et al.<sup>29</sup> suggested an interesting idea that the bathochromic shift of the absorption band of the picrate anion, extracted into the organic phase with a macrocyclic ligand from aqueous metal picrate solutions, serves as a convenient measure for evaluating the ion pair tightness in solution. We thus measured the absorption spectra of alkali picrates in the dichloromethane phase after two-phase solvent extraction. As summarized in Table 1, the  $\lambda_{\text{max}}$  of alkali picrates shift to 377 ~ 378 nm in the presence of **2**. These bathochromic shifts are larger than those induced by cryptands, the ion pairs of which are considered to be nearly "naked".<sup>29</sup> To the best of our knowledge, these bathochromic shifts are the largest among those observed for alkali picrates. As seen from Fig 3, the central cavity of **2** is surrounded by a mesitylene cap and six *tert*-butyl groups and sterically isolated from the solvent medium. Hence, the picrate anion of the **2**·M<sup>+</sup>Pic<sup>-</sup> complex should behave as a highly solvent-separated anion.

The association constants ( $K_{\text{ass}}$ ) could be readily determined from the spectral change of alkali picrates using the Benesi-Hildebrand equation for a 1 : 1 complex.<sup>30</sup> The typical spectral change for Cs<sup>+</sup>Pic<sup>-</sup> is shown in Fig. 7. The plots well satisfied the Benesi-Hildebrand equation with the correlation coefficients > 0.99. Although the solvent (THF) used herein is different from that used in two-phase solvent extraction

(dichloromethane) because of the facile solubilization of alkali picrates into THF, **2** again shows very high Cs<sup>+</sup> selectivity (Table 2). The Cs<sup>+</sup> preference of  $K_{\text{ass}}$  corresponds to ca.  $10^3$ -fold for Rb<sup>+</sup> and more than  $10^3$ -fold for Na<sup>+</sup>.<sup>31</sup> These results establish that the "hole-size selectivity" is satisfactorily operative in the present system featuring a rigid and well-delineated cavity.

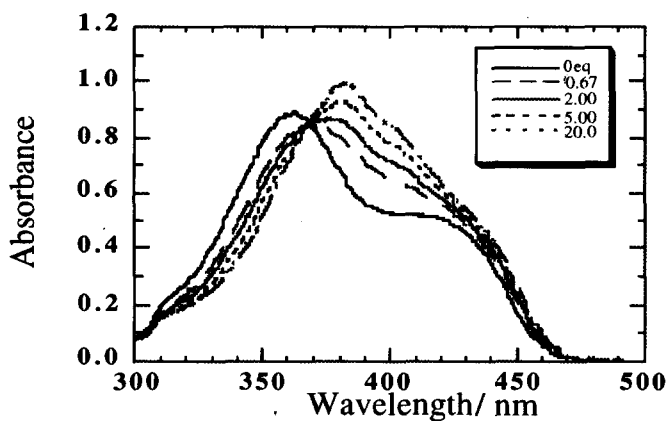


**Fig. 7.** Absorption spectral change of Cs<sup>+</sup>Pic<sup>-</sup> in THF at 25 °C: [Cs<sup>+</sup>Pic<sup>-</sup>] =  $1.00 \times 10^{-5}$  M, [2] (in  $10^{-5}$  M from the bottom to the top at 378 nm) = 0, 0.67, 2.00, 5.00, 20.0, and 30.0.

It is seen from Figs. 1 and 4 indicate that the inner cavity of **2** is nearly C<sub>3</sub>-symmetrical. Although the ion size of ammonium ions (NH<sub>4</sub><sup>+</sup> and RNH<sub>3</sub><sup>+</sup>) is usually comparable with that of K<sup>+</sup>,<sup>32</sup> we expected that they might be bound to this cavity because of their C<sub>3</sub>-symmetrical structure complementary to **2**. Compound **2** also induced the bathochromic shifts for ammonium picrates, from which the  $K_{\text{ass}}$  values could be determined (Table 2). The  $K_{\text{ass}}$  decreases with the increase in the steric bulkiness of R: for example, the  $K_{\text{ass}}$  values for *sec*-BuNH<sub>3</sub><sup>+</sup> and *tert*-BuNH<sub>3</sub><sup>+</sup> are smaller by ca. 29-fold than that for MeNH<sub>3</sub><sup>+</sup>. The  $K_{\text{ass}}$  decrease is rationalized in terms of the steric crowding around the ionophoric inner cavity.

**NMR Studies of Inclusion Complexes.** To obtain further insights into the metal and ammonium binding modes we thoroughly characterized their complexation properties by <sup>1</sup>H NMR spectroscopy. One can regard that the inner cavity of **2** is very unique because the upper hemisphere is covered by three anisole benzene rings and the lower hemisphere is covered by three oxygens in the mesitylene-linked phenyl units: that is, the upper hemisphere is "soft" and the lower hemisphere is "hard".

The temperature-dependent <sup>1</sup>H NMR spectra of a mixture of **2** (2.00 mM) and Cs<sup>+</sup>Pic<sup>-</sup> (1.00 mM) are shown in Fig. 8A. The peaks assignable to the **2**·Cs<sup>+</sup> complex appear separately from those assignable to free

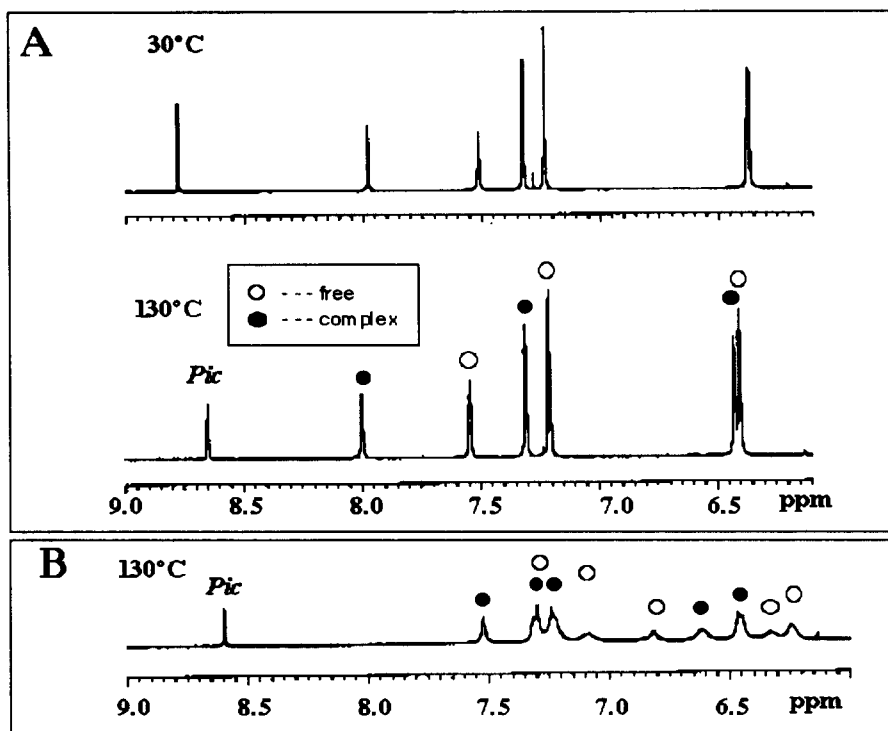


**Fig. 8.** (A) Temperature dependence of partial <sup>1</sup>H NMR spectra (400 MHz) for a mixture of **2** (2.00 mM) and Cs<sup>+</sup>Pic<sup>-</sup> (1.00 mM) in Cl<sub>2</sub>CDCl<sub>2</sub>; although the spectra were measured at every 10 °C, only two of them at 30 °C and 130 °C are shown here. (B) Partial <sup>1</sup>H NMR spectra (130 °C, 400 MHz) of **3** (2.00 mM) and Cs<sup>+</sup>Pic<sup>-</sup> (1.50 mM) in Cl<sub>2</sub>CDCl<sub>2</sub>

**2** even at room temperature and the peak intensities for the complex are always equivalent to the amount of added Cs<sup>+</sup>Pic<sup>-</sup>. The results indicate that the association-dissociation exchange rate is slower than the NMR time-scale and the  $K_{\text{ass}}$  is too large to determine by an NMR spectroscopic method. Surprisingly, the line-broadening of the <sup>1</sup>H NMR signals did not take place even at 130 °C, indicating that the Cs<sup>+</sup> exchange with this rigid and closed cavity is extremely slow. A mixture of **3** (2.00 mM) and Cs<sup>+</sup>Pic<sup>-</sup> (1.00 mM) resulted in the similar temperature-dependent <sup>1</sup>H NMR spectra, but the signals were significantly broadened at 130 °C (Fig. 8B) and the coalescence temperature ( $T_c$ ) for the Cs<sup>+</sup> exchange was approximated to be around 150 °C by its extrapolation. This implies that the Cs<sup>+</sup> exchange with **3** bearing a hole on the upper rim (Fig. 2) is faster than that with **2**.

The chemical shift difference between **2** and **2**·Cs<sup>+</sup> is summarized in Fig. 9. Examination of Fig. 9A reveals that significant Cs<sup>+</sup>-induced down-field shift is observed only for the mesitylene ArH and CH<sub>2</sub> protons

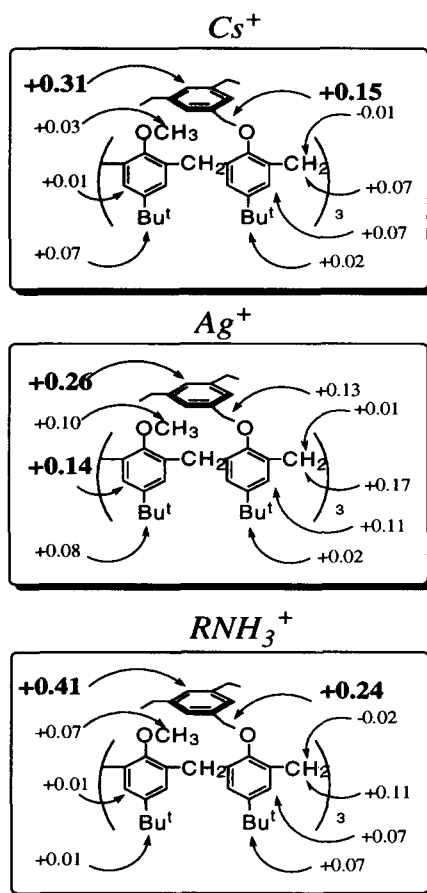


**Fig. 9.** Chemical shift difference between free 2 and  $2 \cdot M^+$  ( $M^+ = Cs^+$ ,  $Ag^+$ , or  $MeNH_3^+$ ) complexes: 400 MHz, 30 °C,  $Cl_2CDCl_2$ ,  $[2] = 2.00$  mM,  $[M^+X^-] = 1.00$  mM. A plus sign (+) denotes a shift to lower magnetic field, whereas a minus sign (-) denotes a shift to higher magnetic field.

( $\Delta\delta = +0.31$  and  $+0.15$  ppm, respectively) whereas the anisole ArH protons covering the upper hemisphere are scarcely affected ( $+0.01$  ppm). It is known that when the cation- $\pi$  interaction operates in the metal binding, the chemical shifts of ArH protons in such complexes mostly move to lower magnetic field.<sup>31,33,34</sup> Thus, the results indicate that the major driving-force for  $Cs^+$  inclusion is the  $Cs^+$ -oxygen interaction with the mesitylene-linked three oxygens whereas methoxy oxygens in the anisole units scarcely contribute to the  $Cs^+$  binding. Here, we expected that both the "hard" lower hemisphere and the "soft" upper hemisphere can act cooperatively to bind  $Ag^+$  because  $Ag^+$  can interact not only with oxygens but also with aromatic  $\pi$ -electrons.<sup>33,35-37</sup> In the  $^1H$

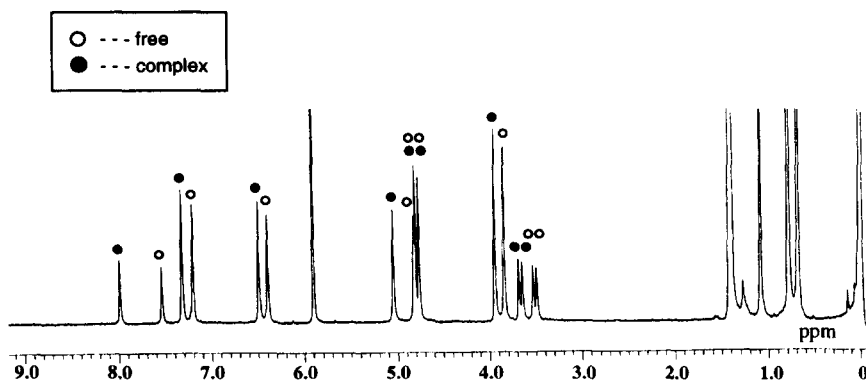


**Fig. 10.** Partial  $^1\text{H}$  NMR spectrum of a mixture of **2** and  $\text{CF}_3\text{SO}_3\text{Ag}$  at  $130\text{ }^\circ\text{C}$ : 400 MHz,  $\text{Cl}_2\text{CDCDCl}_2$ ,  $[\text{2}] = 10.0\text{ mM}$ ,  $[\text{CF}_3\text{SO}_3\text{Ag}] = 5.0\text{ mM}$ .

NMR spectra of a mixture of **2** and  $\text{CF}_3\text{SO}_3\text{Ag}$ , the peaks assignable to the  $\text{2} \cdot \text{Ag}^+$  complex and those assignable to free **2** appeared separately at room temperature. These peaks were neither broadened nor coalesced even at  $130\text{ }^\circ\text{C}$  (Fig. 10), indicating that the  $\text{Ag}^+$  exchange rate is very slow. The chemical shift difference between free **2** and complexed  $\text{2} \cdot \text{Ag}^+$  is summarized in Fig. 9B. It is clearly seen from Fig. 9B that the significant down-field shift is observed not only for the mesitylene ArH and  $\text{CH}_2$  protons ( $\Delta\delta = +0.13 \sim +0.26\text{ ppm}$ ) but also for the anisole ArH protons ( $\Delta\delta = +0.14\text{ ppm}$ ). The  $\delta_{\text{H}}$  for  $\text{H}_{\text{exo}}$  in the  $\text{ArCH}_2\text{Ar}$  methylene protons moves to lower magnetic field by  $+0.17\text{ ppm}$ , indicating that the anisole units rotate upon the  $\text{Ag}^+$  binding. One can thus consider that not only the  $\text{Ag}^+$ -oxygen interaction but also the cation- $\pi$  interaction contributes to the  $\text{Ag}^+$  binding. It is also confirmed (both at  $30\text{ }^\circ\text{C}$  and  $130\text{ }^\circ\text{C}$ ) that the peak intensities of the  $\text{2} \cdot \text{Ag}^+$  complex are always equivalent to the concentration of added  $\text{CF}_3\text{SO}_3\text{Ag}$ . This implies that **2** and  $\text{Ag}^+$  form a very stable 1 : 1 complex.

The NMR studies of the ammonium ion complexes are of particular interest because one can estimate (i) whether the  $\text{C}_3$ -symmetrical architecture of **2** is really effective in the binding of  $\text{C}_3$ -symmetrical ammonium ion guests and (ii) which open space in **2** is used for the alkyl substituents in  $\text{RNH}_3^+$  to penetrate into the cavity. As expected, the peaks assignable to the  $\text{2} \cdot \text{RNH}_3^+$  complexes and those assignable to free **2** appeared separately at room temperature. Neither the line-broadening nor the peak coalescence took place even at  $130\text{ }^\circ\text{C}$ . The results indicate again that the intermolecular exchange rate with  $\text{RNH}_3^+$  guests is very slow. The difference in

**Table 3.** Chemical Shift ( $\delta_{\text{H}}$ ) of the  $2 \cdot \text{RNH}_3^+$  Complexes at 30 °C in  $\text{Cl}_2\text{CDCl}_2$ 

protons	$\delta_{\text{H}}$ /ppm				
	R = Me	Et	<i>n</i> -Pr	<i>n</i> -Bu	<i>tert</i> -Bu
<i>tert</i> -Bu (anisole unit)	0.77	0.79	0.84	0.89	0.90
<i>tert</i> -Bu(mesitylene-linked unit)	1.42	1.42	1.42	1.42	1.41
OMe	3.92	3.92	3.91	3.91	3.91
H <sub>exo</sub> in ArCH <sub>2</sub> Ar	3.68	3.67	3.69	3.69	3.69
H <sub>endo</sub> in ArCH <sub>2</sub> Ar	4.79	4.80	4.81	4.81	4.79
ArOCH <sub>2</sub>	5.11	5.18	5.25	5.29	5.29
ArH (anisole unit)	6.41	6.51	6.62	6.70	6.71
ArH (mesitylene-linked unit)	7.33	7.34	7.35	7.36	7.35
ArH (mesitylene)	8.05	8.22	8.41	8.51	8.48

the chemical shifts between free **2** and  $2 \cdot \text{MeNH}_3^+$  is summarized in Fig. 9C. It is seen from Fig. 9C that the chemical shifts of  $2 \cdot \text{MeNH}_3^+$  are more or less similar to those of  $2 \cdot \text{Cs}^+$ : i.e., the significant down-field shift is observed only for the mesitylene ArH and CH<sub>2</sub> protons. One can thus consider that the major driving-force operating in ammonium guest inclusion is the hydrogen-bonding interaction between three CH<sub>2</sub>OAr oxygens and RNH<sub>3</sub><sup>+</sup> and therein the C<sub>3</sub> complementarity between the host and the guest is an indispensable factor for the effective binding. In this binding mode, it is most reasonable to propose that the alkyl substituent in RNH<sub>3</sub><sup>+</sup> penetrates into the cavity from the upper rim side through the narrow space surrounded by three alternate *tert*-butyl groups in the anisole units. This view is clearly supported by the  $\delta_{\text{H}}$  of the  $2 \cdot \text{RNH}_3^+$  complexes. As shown in Table 3, the bulkiness of R affects not only the chemical shifts of the *tert*-Bu protons in the anisole units but also those of the ArH protons in the anisole units and the mesitylene cap. Assuming the penetration from the upper rim edge, these protons are all located near the bound RNH<sub>3</sub><sup>+</sup>. On the other hand, the  $\delta_{\text{H}}$  values of the residual protons are scarcely changed. It is seen from Table 3 that a large chemical shift jump is observed between EtNH<sub>3</sub><sup>+</sup> and *n*-PrNH<sub>3</sub><sup>+</sup>. Conceivably, EtNH<sub>3</sub><sup>+</sup> is almost included in the cavity whereas the *n*-propyl group in *n*-PrNH<sub>3</sub><sup>+</sup> partially opens up the space surrounded by three alternate *tert*-butyl groups.

**Kinetic Studies of the Metal Association-Dissociation Processes.** It is known that the metal exchange in conventional crown ethers and ionophoric calix[n]arenes occurs in the rate comparable with or faster than an NMR time-scale. In certain macrocycles with a closed ionophoric cavity such as spherands and cavitands, in contrast, the metal exchange occurs more slowly than a human time-scale.<sup>38-40</sup> Although the determination of the kinetic activation parameters which govern unit processes in these host-guest interactions is of great significance, neither of them is suitable to this purpose. The CPK molecular model, theoretical energy-minimization, and X-ray analysis of **2** all suggested that they possess a closed inner cavity delineated by oxygen atoms and  $\pi$ -basic benzene rings, the size of which is comparable with the ion size of  $\text{Cs}^+$ . Although there is no apparent hole for  $\text{Cs}^+$  to get into the cavity (see Fig. 1), the mixture of **2** and  $\text{Cs}^+$  affords a  $2 \cdot \text{Cs}^+$  complex. This implies that **2** creates a "temporary hole" by its breathing molecular motion. In contrast, compound **3** has a permanently-open hole on the upper rim (see Fig. 2). The NMR studies showed that the  $\text{Cs}^+$  exchange rate with **2** is slower by far than the NMR time-scale whereas that with **3** is comparable with the NMR time-scale. Then, how slow are they?

We tentatively followed a complexation process between **2** and  $\text{Cs}^+\text{Pic}^-$  by a conventional spectroscopic method. *Very surprisingly, this process could be easily monitored, the half-lives being 10 ~ 20 sec.*<sup>41b</sup> To confirm that this spectral change is not due to the transition in the mixing process we repeated the same operation using 18-crown-6 or **6** instead of **2**. As expected, the absorbance immediately increased to a new value after the dead-time (ca. 5 sec) and then the time-course remained constant. The kinetic behavior of compound **3** without *tert*-butyl groups on the upper rim was the same as that of 18-crown-6 or **6**. The difference clearly indicates that the shielding of the calix[6]arene cavity by three alternate *tert*-butyl groups is essential for the slow  $\text{Cs}^+$  exchange.

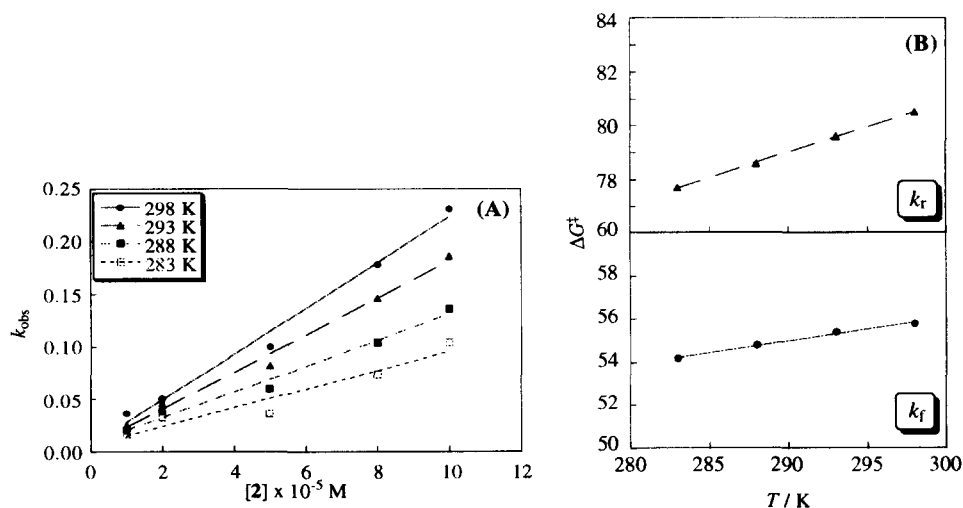


**Fig. 11.** (A) Plots of  $k_{\text{obs}}$  vs.  $[\mathbf{2}]$  for the complexation between **2** and  $\text{Cs}^+\text{Pic}^-$  in THF:  $[\mathbf{2}] = 1.00 \times 10^{-4} \text{ M}$ ,  $[\text{Cs}^+\text{Pic}^-] = 1.00 \times 10^{-5} \text{ M}$ . (B) Plots of  $\Delta G^\ddagger$  vs.  $T$ .

The complexation between **2** and  $\text{Cs}^+\text{Pic}^-$  is an equilibrium reaction, so that the pseudo-first-order rate constant ( $k_{\text{obs}}$ ) under  $[\mathbf{2}] \gg [\text{Cs}^+\text{Pic}^-]$  can be expressed by eq 1,

$$k_{\text{obs}} = k_f [\mathbf{2}] + k_r \quad (1)$$

where  $k_f$  and  $k_r$  are the forward second-order rate constant for the association of **2** and  $\text{Cs}^+\text{Pic}^-$  and the reverse first-order rate constant for the dissociation of  $\mathbf{2} \cdot \text{Cs}^+\text{Pic}^-$ , respectively.<sup>41,42</sup> To determine  $k_f$  and  $k_r$  at 25 °C, the  $k_{\text{obs}}$  values were measured at various **2** concentrations.<sup>41c</sup> The  $k_f$  and the  $k_r$  are the slope and the intercept in the plots of  $k_{\text{obs}}$  vs.  $[\mathbf{2}]$ , respectively. As the linearity of these plots was satisfactorily good ( $\gamma > 0.98$ ), the  $k_f$  could be determined from the slope (Fig. 11A). On the other hand, the  $k_r$  was too small to accurately determine from the intercept. The  $K_{\text{ass}}$  at 25 °C is already determined by a spectroscopic method (Table 2), so that one can calculate the  $k_r$  from the relationship  $K_{\text{ass}} = k_f / k_r$ . We repeated the same measurements and determined  $k_f$  and  $K_{\text{ass}}$  at 10, 15, and 20 °C in addition to 25 °C and then computed  $k_r$  from  $k_f$  and  $K_{\text{ass}}$ . From plots of  $\Delta G^\ddagger$  for  $k_r$

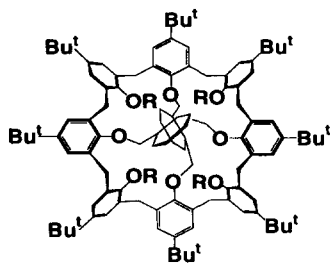
**Table 4.** Thermodynamic Parameters for the Equilibrium and the Reaction between  $\text{Cs}^+\text{Pic}^-$  and **2**, **7a**, and **7b**<sup>a</sup>

	<b>2</b>	<b>7a</b> <sup>b</sup>	<b>7b</b> <sup>b</sup>
$K$ ( $\text{M}^{-1}$ )	$2.1 \times 10^4$	$1.3 \times 10^3$	$1.9 \times 10^4$
$\Delta G^\circ$ (kJ / mol)	-25	-18	-24
$\Delta H^\circ$ (kJ / mol)	-1.3	-0.11	-4.8
$\Delta S^\circ$ (J / K · mol)	78	62	70
$k_f$ ( $\text{M}^{-1}\text{s}^{-1}$ )	1100	520	410
$\Delta G_r^\ddagger$ (kJ / mol)	54	57	58
$\Delta H_r^\ddagger$ (kJ / mol)	25	41	16
$\Delta S_r^\ddagger$ (J / K · mol)	-110	-52	-140
$k_r$ ( $\text{s}^{-1}$ )	0.047	0.38	0.021
$\Delta G_r^\ddagger$ (kJ / mol)	79	75	83
$\Delta H_r^\ddagger$ (kJ / mol)	27	41	21
$\Delta S_r^\ddagger$ (J / K · mol)	-200	-110	-200

<sup>a</sup>  $K$ ,  $k_f$ , and  $k_r$  are those at 298 K

<sup>b</sup> Cited from reference 41b

and  $k_f$  vs.  $T$ <sup>41c</sup> we obtained  $\Delta H^\ddagger$  and  $\Delta S^\ddagger$  for the forward reaction and the reverse reaction (Fig. 11B). The results are summarized in Table 4. It was found that van't Hoff plots for the association equilibrium result in a good linear relationship.<sup>41c</sup> The  $\Delta H^\circ$  and  $\Delta S^\circ$  values were determined from the slope ( $-\Delta H^\circ / R$ ) and the intercept ( $\Delta S^\circ / R$ ), respectively, by a least-squares procedure. The results are also summarized in Table 4. In Table 4 we include thermodynamic parameters obtained from doubly-bridged calix[8]arenes (**7a** and **7b**)<sup>41b</sup> in order to understand these thermodynamic parameters by extensive comparison.



**7a: R = Me**

**7b: R = Et**

One can raise a number of important and novel features of the  $\text{Cs}^+$  complexation process disclosed for the first time by the kinetic studies of capsule-like calix[n]arenes. Firstly, the  $k_f$  values are different only to a smaller extent (only 2.7-fold between largest **2** and smallest **7b**) whereas the  $k_r$  values are largely different (18-fold between largest **7a** and smallest **7b**). The result implies that the  $K_{\text{ass}}$  is governed mainly by the decrease in the  $k_r$ . This tendency is in line with that of the metal complexation behavior in crown ethers and cryptands which can be obtained only by the use of a stopped-flow method or a  $T$ -jump method.<sup>44,45,46</sup> Secondly and most intriguingly, the  $\Delta S^\circ$  values are all positive and the order of the  $K_{\text{ass}}$  is consistent with that of  $\Delta S^\circ$  (i.e., **2** > **7b** > **7a**) but not with that of  $-\Delta H^\circ$  (**7b** > **2** > **7a**). In general, the metal complexation process is driven by the negative (favorable) enthalpy change and accompanies the negative (unfavorable) entropy change.<sup>47</sup> In contrast, the present results indicate that the major driving-force for metal inclusion is not the  $\Delta H^\circ$  term but the  $\Delta S^\circ$  term and the final complexation state is more entropically-favorable than the initial state. The careful survey of the past literatures teaches us that such an unusual positive  $\Delta S^\circ$  change results when the ionophore is sterically rigid and the metal complexation consumes the considerable desolvation energy.<sup>48</sup> As demonstrated by <sup>1</sup>H NMR spectroscopy and theoretical calculations, these compounds are sterically very rigid and exactly can be classified into this class of ionophores.<sup>42</sup> Thirdly, the structural difference between **7a** and **7b** is the *O*-substituent

(methyl or ethyl). Examination of the activation parameters reveals that **7b** with ethyl substituents possesses the more favorable  $\Delta H^\ddagger$  term and the more unfavorable  $\Delta S^\ddagger$  term both for the forward and the reverse reaction than **7a** with methyl substituents. This indicates that also in **2**, the steric crowding increases the  $-\Delta S^\ddagger$  term, which suppressed the  $\text{Cs}^+$  exchange and eventually enabled us to determine the reaction rates with a conventional spectroscopic method.

The present calix[n]arene system is a very rare example in which the metal complexation process can be followed by a conventional spectroscopic method. By taking this advantage, one can readily determine the activation parameters. The results established that the metal complexation equilibrium in rigid calix[n]arenes is crucially governed by the entropy term but not by the enthalpy term, being different from the concept believed so far. This is a new thermodynamic insight into the metal inclusion chemistry and useful as a new concept in ionophore design.

## CONCLUSION

The present study reports the thorough characterizations of a calix[6]arene with a unique unimolecularly-closed ionophoric cavity. It showed the high selectivity toward  $\text{Cs}^+$ , the high affinity with  $\text{Ag}^+$ , and the moderate affinity with  $\text{RNH}_3^+$  (probably because of  $C_3$ -symmetrical complementarity). Furthermore, the  $\text{Cs}^+$  association-dissociation processes could be followed by a conventional spectroscopic method. We believe that compound **2** is one of such "more rigid and conformationally-defined calix[6]arene analogs"<sup>2c</sup> and useful to understand the guest inclusion properties from both spectroscopic and thermodynamic viewpoints.

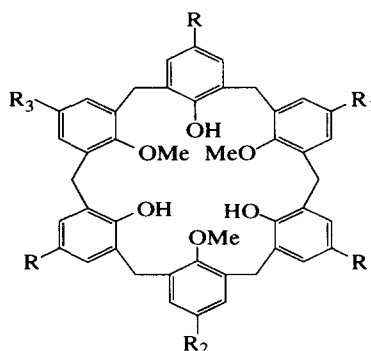
## EXPERIMENTAL

**Materials.** Preparation of compound **2** has been described.<sup>17b</sup>

**37,39,41-Trimethoxy-38,40,42-trihydroxycalix[6]arene (8).** 5,11,17,23, 29,35-Hexa-*tert*-butyl-37,39,41-trimethyl-38,40,42-trihydroxycalix[6]arene<sup>7c,17b,21,22</sup> (150 mg, 0.15 mmol) in toluene (30 mL) was treated with  $\text{AlCl}_3$  (1.2 g, 9.0 mmol) at room temperature under a nitrogen atmosphere. After 4 h, the reaction was stopped by the addition of aqueous 1 M HCl solution (5 mL). The resultant mixture was extracted with chloroform. The chloroform layer was separated, washed three times with water, and dried over  $\text{MgSO}_4$ . The solution was concentrated to dryness and the residual solid was subjected to column chromatography (silica gel, dichloromethane). We separated the eluent into six fractions. We could isolate **10** and **11** from the fourth and the fifth fraction, respectively, which gave  $R_f = 0.35$  and  $0.40$  on the TLC plate (silica gel, dichloromethane). On the other hand, the  $^1\text{H}$  NMR measurement showed that the sixth fraction (with  $R_f = 0.30$ ) contains two compounds. They could be separated by a preparative TLC method (silica gel, ethyl acetate:

hexane = 1 : 2 v/v) :  $R_f$  = 0.35 for **9** and 0.30 for **8**. **11**: yield 15%;  $^1\text{H NMR}$  ( $\text{CDCl}_3$ , 25 °C)  $\delta$  1.05 (*t*-Bu, s, 27H), 3.51 ( $\text{OCH}_3$ , s, 9H), 3.91 ( $\text{ArCH}_2\text{Ar}$ , s, 12H), 6.73, 6.92, and 7.00 ( $\text{ArH}$ , t, s, and d, respectively, 3H, 6H, and 3H, respectively), 6.94 (OH, s, 3H). **10**: yield 15%;  $^1\text{H NMR}$  ( $\text{CDCl}_3$ , 25 °C)  $\delta$  1.06 (*t*-Bu, s, 18H), 3.43 and 3.70 ( $\text{OCH}_3$ , s each, 6H and 3H, respectively), 3.89, 3.92 and 3.94 ( $\text{ArCH}_2\text{Ar}$ , s each, 4H each), 6.7–7.1 ( $\text{ArH}$  and OH, m, 19H). **9**: yield 10%;  $^1\text{H NMR}$  ( $\text{CDCl}_3$ , 25 °C)  $\delta$  1.06 (*t*-Bu, s, 18H), 3.48 and 3.57 ( $\text{OCH}_3$ , s each, 3H and 6H, respectively), 3.90, 3.93 and 3.94 ( $\text{ArCH}_2\text{Ar}$ , s each, 4H each), 6.7–7.3 ( $\text{ArH}$  and OH, m, 20H). **8**: yield 10%;  $^1\text{H NMR}$  ( $\text{CDCl}_3$ , 25 °C)  $\delta$  3.57 ( $\text{OCH}_3$ , s, 9H), 3.93 ( $\text{ArCH}_2\text{Ar}$ , s, 12H), 6.6–7.1 ( $\text{ArH}$  and OH, m, 21H).

**Compound 3**. This compound was synthesized from **8** and 1,3,5-tris(bromomethyl)benzene under high-dilution conditions in a manner similar to that described for **2**.<sup>17b</sup> Finally, the product was purified by reprecipitation from chloroform to methanol : mp > 320 °C, yield 90%; IR(Nujol) no  $\nu_{\text{OH}}$ ;  $^1\text{H NMR}$  ( $\text{CDCl}_3$ , 25 °C)  $\delta$  3.71 and 4.78 ( $\text{ArCH}_2\text{Ar}$ , d each,  $J$  = 16.5 Hz for all peaks, 2H each), 3.93 ( $\text{OCH}_3$ , s, 3H), 4.54 ( $\text{ArOCH}_2$ , s, 2H), 6.29, 6.41, 7.12, and 7.27 ( $\text{ArH}$ (calixarene), d, t, t, d, respectively, 2H, 1H, 2H, 1H, respectively), 6.82 ( $\text{ArH}$ (cap), s, 1H).



**8** :  $R = R_1 = R_2 = R_3 = \text{H}$

**9** :  $R = R_1 = R_2 = \text{H}$ ,  $R_3 = t\text{-Bu}$

**10** :  $R = R_1 = \text{H}$ ,  $R_2 = R_3 = t\text{-Bu}$

**11** :  $R = \text{H}$ ,  $R_1 = R_2 = R_3 = t\text{-Bu}$

**X-ray Crystal Structure Determination of 2**. Colorless crystal were obtained by recrystallization from *p*-xylene. The crystal structure of **2** was determined by X-ray diffraction. Crystal data:  $\text{C}_{94}\text{H}_{116}\text{O}_6$ , triclinic, space group  $\text{P1}(\#2)$ ;  $a = 19.524(2)$  Å,  $b = 21.541(2)$  Å,  $c = 10.5281(5)$  Å,  $\alpha = 19.524(2)$  °,  $\beta =$

19.524(2) °,  $\gamma = 19.524(2)$  °;  $V = 4310.4(5)$  Å<sup>3</sup>;  $Z = 2$ ;  $D_{\text{calc}} = 1.034$  g cm<sup>-3</sup>;  $m = 4.81$  cm<sup>-1</sup>. Reflections were measured at 293 K in the  $w$ - $2\theta$  scan mode [ $51.26^\circ < 2\theta < 55.99^\circ$ ], using Cu-K $\alpha$  radiation ( $\lambda = 1.54178$  Å). The structure was solved by the direct methods (SAPI91) and refined with full-matrix least-square methods. A total of 6715 reflections with  $I > 3.00\sigma$  was used in the refinement. The R factors were  $R = 19.8\%$  and  $R_w = 25.4\%$ . All calculation were performed with teXsan crystallographic software package of Molecular Structure Corporation.

**Solvent Extraction.** Two-phase solvent extraction of alkali picrates was carried out between water (5 mL, [alkali picrate] =  $1.00 \times 10^{-4}$  M, [MOH] =  $1.00 \times 10^{-4}$  M) and dichloromethane (5 mL, [**2**] =  $1.00 \times 10^{-3}$  M). The two-phase mixture was shaken for 12 h at 25 °C. The extractability was determined spectrophotometrically from the decrease in the absorbance of the picrate ion in the aqueous phase.

**Kinetics.** The reaction rate for inclusion of Cs<sup>+</sup>Pic<sup>-</sup> into **2** was evaluated under the pseudo-first-order conditions where **2** exists in great excess over Cs<sup>+</sup>Pic<sup>-</sup> ( $1.00 \times 10^{-5}$  M). A THF solution (3 mL) containing Cs<sup>+</sup>Pic<sup>-</sup> was equilibrated to the desired temperature. Then, a THF solution (ca. 30 mL) containing **2** was injected from a micro-syringe. After rapidly shaking this mixture, the cuvette was returned into the spectrophotometer and the time-course of the reaction was followed at 390 nm. It took about 5 sec from the injection of the **2** solution to the start of the measurement. The time (after 5 sec) vs.  $A_{390}$  plots satisfied the first-order equation with  $\gamma > 0.98$ .

**Miscellaneous.** <sup>1</sup>H NMR, VT-NMR, UV-Vis, and kinetic UV-Vis spectroscopic measurements were carried out with a Bruker AC 250P spectrophotometer, a JEOL GSX-400 spectrometer, a Shimadzu UV-160 spectrometer, and HITACHI U-3000 spectrometer respectively. The calculation of X-ray crystal structure determination was performed with teXsan crystallographic software package of Molecular Structure Corporation. MM3(92) calculation was performed on a UNIX workstation system: SUN 4/2 GX-IRIS 4D/35G.

#### ACKNOWLEDGMENT

We are indebted to Dr. Takaaki Harada for theoretical calculations using MM3 (92). This work is supported by Grant-in-Aid from the Ministry of Education, Science and Culture.

#### REFERENCES

1. For comprehensive reviews see (a) Gutsche, C. D. In *Calixarenes*; Royal Society of Chemistry: Cambridge, 1989. (b) Vicens, J.; Böhmer, V. (Eds.) In *Calixarenes*; Kluwer Academic Press: Dordrecht, 1991. (c) Shinkai, S. *Bioorg. Chem. Front.* **1990**, *1*, 161. (d) Böhmer, V. *Angew. Chem. Int. Ed. Engl.* **1995**, *34*, 713. (e) Shinkai, S. *Tetrahedron* **1993**, *49*, 8933. (f) Otsuka, H.; Shinkai S. *Supramol. Sci.* **1996**, *3*, 189.

2. (a) Gutsche, C. D.; Levine, J. A. *J. Am. Chem. Soc.* **1982**, *104*, 2652. (b) Gutsche, C. D.; Lin, L.-G. *Tetrahedron* **1986**, *42*, 1633. (c) Gutsche, C. D.; Alam, I. *Ibid.* **1988**, *44*, 4689.
3. (a) Almi, M.; Arduini, A.; Casnati, A.; Pochini, A.; Ungaro, R. *Tetrahedron* **1989**, *45*, 2177. (b) Arduini, A.; Manfredi, G.; Pochini, A.; Sicuri, A. R.; Ungaro, R. *J. Chem. Soc., Chem. Commun.* **1991**, 936.
4. (a) Verboom, W.; Durie, A.; Egberink, R. J. M.; Asfari, Z.; Reinhoudt, D. N. *J. Org. Chem.* **1992**, *57*, 1313. (b) van Loon, J. -D.; Arduini, A.; Coppi, L.; Verboom, W.; Pochini, A.; Ungaro, R.; Harkema, S.; Reinhoudt, D. N. *Ibid.* **1990**, *55*, 5639.
5. (a) Shinkai, S.; Mori, S.; Koreishi, H.; Tsubaki, T.; Manabe, O. *J. Am. Chem. Soc.* **1986**, *108*, 2409. (b) Shinkai, S.; Araki, K.; Tsubaki, T.; Manabe, O. *J. Chem. Soc., Perkin Trans. 1* **1987**, 2297. (c) Arimura, T.; Nagasaki, T.; Shinkai, S.; Manabe, O. *J. Org. Chem.* **1989**, *54*, 3767. (d) Komori, T.; Shinkai, S. *Chem. Lett.* **1992**, 901.
6. (a) Gutsche, C. D.; Bauer, L. J. *J. Am. Chem. Soc.* **1985**, *107*, 6059. (b) Gutsche, C. D.; Reddy, P. A. *J. Org. Chem.* **1991**, *56*, 4783. (c) Kanamathareddy, S.; Gutsche, C. D. *J. Org. Chem.* **1992**, *57*, 3160.
7. (a) Bocchi, V.; Foina, D.; Pochini, A.; Ungaro, R.; Andreetti, G. D. *Tetrahedron* **1982**, *38*, 373. (b) Arduini, A.; Pochini, A.; Reverberi, S.; Ungaro, R.; Andreetti, G. D.; Ugozzoli, F. *Ibid.* **1986**, *42*, 2089. (c) Casnati, A.; Minari, P.; Ungaro, R. *J. Chem. Soc., Chem. Commun.* **1991**, 1413. (d) Arduini, A.; Casnati, A.; Fabbi, M.; Minari, P.; Pochini, A.; Sicuri, A. R.; Ungaro, R. *Supramol. Chem.* **1993**, *1*, 235.
8. (a) Groenen, L. C.; van Loon, J. -D.; Verboom, W.; Harkema, S.; Casnati, A.; Ungaro, R.; Pochini, A.; Ugozzoli, F.; Reinhoudt, D. N. *J. Am. Chem. Soc.* **1991**, *113*, 1285. (b) Verboom, W.; Datta, S.; Asfari, Z.; Harkema, S.; Reinhoudt, D. N. *J. Org. Chem.* **1992**, *57*, 5394. (c) Groenen, L. C.; Ruel, B. H. M.; Casnati, A.; Timmerman, P.; Verboom, W.; Harkema, S.; Pochini, A.; Ungaro, R.; Reinhoudt, D. N. *Tetrahedron Lett.* **1991**, *32*, 2675.
9. (a) Iwamoto, K.; Araki, K.; Shinkai, S. *J. Org. Chem.* **1991**, *56*, 4955. (b) *Idem Tetrahedron* **1991**, *47*, 4325. (c) Iwamoto, K.; Shinkai, S. *J. Org. Chem.* **1992**, *57*, 7066. (d) Shinkai, S.; Fujimoto, K.; Otsuka, T.; Ammon, H. L. *Ibid.* **1992**, *57*, 1516. (e) Iwamoto, K.; Shimizu, H.; Araki, K.; Shinkai, S. *J. Am. Chem. Soc.* **1993**, *115*, 3997.
10. McKervey, M. A.; Seward, E. M.; Ferguson, G.; Ruhl, B.; Harris, S. *J. Chem. Soc., Chem. Commun.* **1985**, 388.
11. Arnaud-Neu, F.; Collins, E. M.; Deasy, M.; Ferguson, G.; Harris, S. J.; Kaitner, B.; Lough, A. J.; McKervey, M. A.; Marques, E.; Ruhl, B. L.; Schwing Weill, M. J.; Seward, E. M. *J. Am. Chem. Soc.* **1989**, *111*, 8681.
12. Arimura, T.; Kubota, M.; Matsuda, T. Manabe, O.; Shinkai, S. *Bull. Chem. Soc. Jpn.* **1989**, *62*, 1674.
13. Araki, K.; Iwamoto, K.; Shinkai, S.; Matsuda, T. *Chem. Lett.* **1989**, 1747.
14. Grynszpan, F.; Aleksyuk, O.; Biali, S. E. *J. Chem. Soc., Chem. Commun.* **1993**, 13.
15. (a) Kanamathareddy, S.; Gutsche, C. D. *J. Am. Chem. Soc.* **1993**, *115*, 6572. (b) Kanamathareddy, S.; Gutsche, C. D. *J. Org. Chem.* **1994**, *59*, 3871.

16. (a) Araki, K.; Akao, K.; Otsuka, H.; Nakashima, K.; Inokuchi, F.; Shinkai, S. *Chem. Lett.* **1994**, 1251.  
(b) Takeshita, M.; Nishio, S.; Shinkai, S. *J. Org. Chem.* **1994**, 59, 4032.
17. (a) Otsuka, H.; Araki, K.; Shinkai, S. *J. Org. Chem.* **1994**, 59, 1542. (b) Otsuka, H.; Araki, K.; Matsumoto, H.; Harada, T.; Shinkai, S. *J. Org. Chem.* **1995**, 60, 4862.
18. It has been shown that a 1,3-bridged calix[6]arene does not racemize using a chiral capped calix[6]arene; since ring inversion is obligatorily accompanied by racemization, one can estimate whether this calix[6]arene ring is truly immobilized: see Otsuka, H.; Shinkai, S. *J. Am. Chem. Soc.* **1996**, 118, 4271.
19. For calixarene-based cage molecules see: (a) Timmerman, P.; Nierop, K.G.A.; Verboom, W.; van Veggel, F.C.J.M.; van Hoorn, W.D.; Reinhoudt, D.N. *Chem. Eur. J.* **1995**, 1, 132. (b) Timmerman, P.; Verboom, W.; van Veggel, F.C.J.M.; van Duynhoven, J.P.M.; Reinhoudt, D.N. *Angew. Chem. Int. Ed. Engl.* **1994**, 33, 2345. (c) Mogck, O.; Paulus, E. F.; Böhmer, V.; Thondorf, I.; Vogt, W. *J. Chem. Soc., Chem. Commun.*, **1996**, 2553. (d) Hamman, B. C.; Shimizu, K. D.; Rebek, Jr., J. *Angew. Chem. Int. Ed. Engl.*, **1996**, 35, 1326.
20. (a) Harada, T.; Rudzinski, J. M.; Osawa, E.; Shinkai, S. *Tetrahedron* **1993**, 49, 5941. (b) Harada, T.; Otsuka, F.; Shinkai, S. *Ibid.* **1944**, 50, 13377. (c) Harada, T.; Shinkai, S. *J. Chem. Soc., Perkin Trans. 2* **1995**, 1. For computational studies of calix[n]arenes by other groups see (d) Grootenhuis, P. D. J.; Kollman, P. A.; Groenen, L. C.; Reinhandt, D. N.; van Hummel, G. J.; Ugozzoli, F.; Andreetti, G. D. *J. Am. Chem. Soc.* **1990**, 112, 4165. (e) Fischer, S.; Grootenhuis, P. D. J.; Groenen, L. C.; van Hoorn, W. P.; van Veggel, F. C. J. M.; Reinhandt, D. N.; Karplus, M. *J. Am. Chem. Soc.* **1995**, 117, 1611. (f) Roger, J.; Bayard, F.; Decoret, C. *J. Chim. Phys.* **1990**, 87, 1695. (g) Miyamoto, S.; Kollman, P. A. *J. Am. Chem. Soc.* **1992**, 114, 3668. (h) Dohan, E.; Biali, S. E., *J. Org. Chem.* **1991**, 56, 7269.
21. (a) Andreetti, C. D.; Calestani, G.; Ugozzoli, F.; Arduini, A.; Ghidini, E.; Pochini, A.; Ungaro, R. *J. Inclusion Phenom.* **1987**, 5, 123. (b) Janssen, R. G.; Verboom, W.; Reinhoudt, D. N.; Casnati, A.; Freriks, M.; Pochini, A.; Ugozzoli, F.; Ungaro, R.; Nieto, P. M.; Carramolino, M.; Cuevas, F.; Prados, P.; de Mendoza, J. *Synthesis*, **1993**, 380.
22. This range is changeable, depending on the rotation of *tert*-Bu groups.
23. Otsuka, H.; Araki, K.; Shinkai, S. *Chem. Express* **1993**, 8, 479. (b) Otsuka, H.; Araki, K.; Sakaki, T.; Nakashima, N.; Shinkai, S. *Tetrahedron Lett.* **1993**, 34, 7275.
24. van Duynhoven, J. P. M.; Janssen, R. G.; Verboom, W.; Franken, S. M.; Casnati, A.; Pochini, A.; Ungaro, R.; de Mendoza, J.; Nieto, P. M.; Prados, P.; Reinhoudt, D. N. *J. Am. Chem. Soc.* **1994**, 116, 5814.
25. Other examples for capping of calix[6]arenes (although their purposes are not necessarily immobilization of the conformation): (a) Janssen, R. G.; Verboom, W.; van Duynhoven, J. P. M.; van Velzen, E. J. J.; Reinhoudt, D. N. *Tetrahedron Lett.* **1994**, 35, 6555. (b) Kraft, K.; Böhmer, V.; Vogt, W.; Ferguson, G.; Gallagher, J. F. *J. Chem. Soc., Perkin Trans. 1* **1994**, 1221.
26. Andreetti, G. D.; Calestani, G.; Ugozzoli, F.; Arduini, A.; Ghidini, E.; Pochini, A.; Ungaro, R. *J. Incl. Phenom.* **1987**, 5, 123.
27. Chang, S.-K.; Cho, I. *J. Chem. Soc., Perkin Trans. 1* **1986**, 211.

28. (a) Sakaki, T.; Harada, T.; Deng, G.; Kawabata, H.; Kawahara, Y.; Shinkai, S. *J. Incl. Phenom.* **1992**, *14*, 285 and references cited therein. (b) Sakaki, T.; Harada, T.; Kawahara, Y.; Shinkai, S. *Ibid.* **1994**, *17*, 377.
29. Inoue, Y.; Fujiwara, C.; Wada, K.; Hakushi, T. *J. Chem. Soc., Chem. Commun.* **1987**, 393.
30. Benesi, H. A.; Hildebrand, H. *J. Am. Chem. Soc.* **1949**, *71*, 2703.
31. A Cs<sup>+</sup>-selective ionophore is also designed from 1,3-alternate calix[4]crown, in which both the oxygen-metal interaction and the cation- $\pi$  interaction contribute to the Cs<sup>+</sup>-binding: (a) Ungaro, R.; Casnati, A.; Ugozzoli, F.; Pochini, A.; Dozol, J.-F.; Hill, C.; Rouquette, H. *Angew. Chem. Int. Ed. Engl.* **1994**, *33*, 1506. (b) Casnati, A.; Pochini, A.; Ungaro, R.; Ugozzoli, F.; Arnaud, F.; Fanni, S.; Schwing, M.-J.; Egberink, R. J. M.; de Jong, F.; Reinhoudt, D. N. *J. Am. Chem. Soc.* **1995**, *117*, 2767. (c) Arnaud-Neu, F.; Asfari, Z.; Souley, B.; Viceus, J. *New J. Chem.* **1996**, *20*, 453.
32. Gokel, G. *Crown Ethers & Cryptands*; The Royal Society of Chemistry: Cambridge, 1991.
33. (a) Ikeda, A.; Shinkai, S. *Tetrahedron Lett.* **1992**, *33*, 7385. (b) Idem, *J. Am. Chem. Soc.* **1994**, *116*, 3102 and references cited therein. (c) Ikeda, A.; Tsuzuki, H.; Shinkai, S. *J. Chem. Soc., Perkin Trans. 2* **1994**, 2073.
34. Casnati, A.; Pochini, A.; Ungaro, R.; Ugozzoli, F.; Arnaud, F.; Fanni, S.; Swing, M.-J.; Egberink, R. J. M.; de Jong, F.; Reinhoudt, D. N. *J. Am. Chem. Soc.* **1995**, *117*, 2767.
35. Vögtle, F.; Gross, J.; Seel, C.; Nieger, M. *Angew. Chem. Int. Ed. Engl.* **1992**, *31*, 1069 and references cited therein. For the  $\pi$ -donor participation see: (a) Iyoda, M.; Kuwatani, Y.; Yamauchi, T.; Oda, J. *J. Chem. Soc., Chem. Commun.* **1988**, 65. (b) Leokes, R.; Vögtle, F. *Chem. Ber.* **1983**, *116*, 215. (c) Pierre, J.-L.; Baret, P.; Chautemps, P.; Armand, M. *J. Am. Chem. Soc.* **1981**, *103*, 2986. (d) Kang, H. C.; Hanson, A. W.; Eaton, B.; Boekelheide, V. *Ibid.* **1985**, *107*, 1979. (e) Heitzler, F. R.; Hopf, H.; Jones, P. G.; Bubenitschek, P.; Lehne, V. *J. Org. Chem.* **1993**, *58*, 2781. (f) Gano, J. E.; Subramaniam, G.; Birnbaum, R. *Ibid.* **1990**, *55*, 4760.
36. For the  $\pi$ -donor participation see: (a) Iyoda, M.; Kuwatani, Y.; Yamauchi, T.; Oda, J. *J. Chem. Soc., Chem. Commun.* **1988**, 65. (b) Leokes, R.; Vögtle, F. *Chem. Ber.* **1983**, *116*, 215. (c) Pierre, J.-L.; Baret, P.; Chautemps, P.; Armand, M. *J. Am. Chem. Soc.* **1981**, *103*, 2986. (d) Kang, H. C.; Hanson, A. W.; Eaton, B.; Boekelheide, V. *Ibid.* **1985**, *107*, 1979. (e) Heitzler, F. R.; Hopf, H.; Jones, P. G.; Bubenitschek, P.; Lehne, V. *J. Org. Chem.* **1993**, *58*, 2781. (f) Gano, J. E.; Subramaniam, G.; Birnbaum, R. *Ibid.* **1990**, *55*, 4760.
37. For a theoretical consideration of the cation- $\pi$  interaction see Dougherty, D. A. *Science* **1996**, *271*, 163.
38. Cram, D. J. *Science*, **1983**, *219*, 1177.
39. Dijkstra, P. J.; Brunink, J. A. J.; Bugge, K.-E.; Reinhoudt, D. N.; Harkema, S.; Ungaro, R.; Ugozzoli, F.; Ghidini, E. *J. Am. Chem. Soc.*, **1989**, *111*, 7567.
40. Cram, D. J.; Cram, J. M. *In Container Molecules and Their Guests*; Royal Society of Chemistry: Cambridge, 1994.

41. (a) Shinkai, S.; Tamaki, K.; Kunitake, T. *Makromol. Chem.* **1977**, *178*, 133. (b) Preliminary communication for the kinetic studies: Suzuki, Y.; Otsuka, H.; Ikeda, A.; Shinkai, S. *Tetrahedron Lett.* **1997**, *38*, 421. (c) For plots used to determine kinetic and thermodynamic parameters see Ref. 41b.
42. Lindquist, R. N.; Cordes, E. H. *J. Am. Chem. Soc.* **1968**, *90*, 1269.
43. Cox, B. G.; van Truong, N.; Schneider, H. *J. Am. Chem. Soc.* **1984**, *106*, 1273 and references cited therein.
44. Graves, H. P.; Detellier, C. *J. Am. Chem. Soc.* **1988**, *110*, 6019.
45. Christensen, J. J.; Eatouch, D. L.; Izatt, R. M. *Chem. Rev.* **1974**, *74*, 351.
46. Izatt, R. M.; Pawlak, K.; Bradshaw, J. S. *Chem. Rev.* **1991**, *91*, 1721.
47. Lehn, J.-M.; Sauvage, J. P. *J. Chem. Soc., Chem. Commun.* **1971**, 440.
48. (a) Inoue, Y.; Hakushi, T.; Liu, Y.; Tong, L.-H.; Shen, B.-J.; Jin, D.-S. *J. Am. Chem. Soc.* **1993**, *115*, 475. (b) Iwema Bakker, W. I.; Verboom, W.; Reinhoudt, D. N. *J. Chem. Soc., Chem. Commun.* **1994**, 71. (c) Arnaud-Neu, F.; Arnecke, R.; Bohmer, V.; Fanni, S.; Gordon, J. L. M.; Schwing-Weill, M.-J.; Vogt, W. *J. Chem. Soc., Perkin Trans. 2*, **1996**, 1855. (d) Casnati, A.; Pochini, A.; Ungaro, R.; Ugozzoli, F.; Arnaud, F.; Fanni, S.; Schwing, M.-J.; Egberink, R. J. M.; de Jong, F.; Reinhoudt, D. N. *J. Am. Chem. Soc.* **1995**, *117*, 2767.